

Growth Pathways of Metallocarbohedrenes: Cagelike or Cubic?

Lai-Sheng Wang¹ and Hansong Cheng²

¹Department of Physics, Washington State University, Richland, Washington 99352
and EMSL, MS K2-14, Pacific Northwest National Laboratory, Richland, Washington 99352
²Air Products and Chemicals, Inc., 7201 Hamilton Boulevard, Allentown, Pennsylvania 18195

(Received 24 January 1997)

A novel layer-by-layer cubic growth pathway involving C_2 dimers is advanced for large titanium carbide clusters based on observation of new magic numbers in the anions. This growth mechanism explains uniquely all the magic numbers in a multicage growth model previously proposed for large metal carbide clusters, suggesting that the cubic structures, characteristic of the bulk carbide lattices, dominate growth of the large carbide clusters. Experimental and theoretical evidence indicates that the cubic layered growth with C_2 dimers can lead to a new type of highly stable one-dimensional quantum wires. [S0031-9007(97)02977-3]

PACS numbers: 61.46.+w, 31.15.Ew, 33.60.-q, 36.40.Mr

Metcars ($M_8C_{12}^+$, M = transition metal atoms) were discovered a few years ago as a new class of stable molecular clusters by Castleman and co-workers [1]. These clusters, observed as prominent (magic) peaks in mass spectra of laser vaporization experiments [1,2], were proposed to have a dodecahedral structure with a T_h point group symmetry, a cagelike molecular shape similar to the fullerenes [3]. They were observed to form preferentially for the early transition metals (Ti, V, Cr, Zr, Nb, Mo, and Hf) with $Ti_8C_{12}^+$ being the most prototypical [1,2]. If made in bulk quantity, the metcars are expected to exhibit novel and rich chemical and physical properties because of the transition metals in the molecular structures. Unlike the fullerenes that grow by expanding the cage, however, Wei *et al.* proposed that the large carbide clusters follow a multicage growth path, based on their observation of prominent cluster cations in Zr carbide clusters [4]. Pilgrim and Duncan subsequently showed that Ti, V, and Zr carbide cluster cations all form cubic structures beyond the $M_8C_{12}^+$ metcars [5], much like the bulk cubic crystal lattice. Besides these paradoxical observations, the growth pathways of the metcars remain a central unresolved question, despite extensive theoretical [6–9] and experimental effort [10–14].

In this Letter, we present observation of new magic numbers in the anion mass spectra of titanium carbide clusters, including $Ti_{13}C_{22}^-$ which corresponds to the composition of a double cage in the multicage growth model [4]. In contrast to the double-cage structure, however, we found $Ti_{13}C_{22}$ to have an unusual cubic structure, with eight C_2 dimers occupying the eight cube corners [Fig. 1(a)]. This finding, together with evidence from smaller magic clusters and theoretical calculations, suggests a layer-by-layer cubic growth pathway for the titanium carbide clusters. This cubic-layered growth mechanism can account for all the magic numbers assigned previously to the multicages. Our quantum-mechanical calculations further show that continued growth of these cubic clusters involving C_2 dimers will

result in highly stable structures that can form a novel type of one-dimensional quantum wire.

The experimental apparatus used consists of a laser vaporization cluster source, a time-of-flight mass spectrometer, and a magnetic-bottle photoelectron analyzer that allows the electronic structure of size-selected clusters to be obtained [15]. A pure Ti target is vaporized with a 10 mJ laser pulse (532 nm) and a helium carrier gas containing 5% CH_4 . The plasma reactions between titanium and the CH_4 produce a series of Ti_xC_y clusters in both neutral and charged states. Figure 2 shows an anion mass spectrum of the titanium carbide clusters. Surprisingly, the anticipated metcar Ti_8C_{12} and the cubic $Ti_{14}C_{13}$ cluster so prominent in the cation channel are missing from the

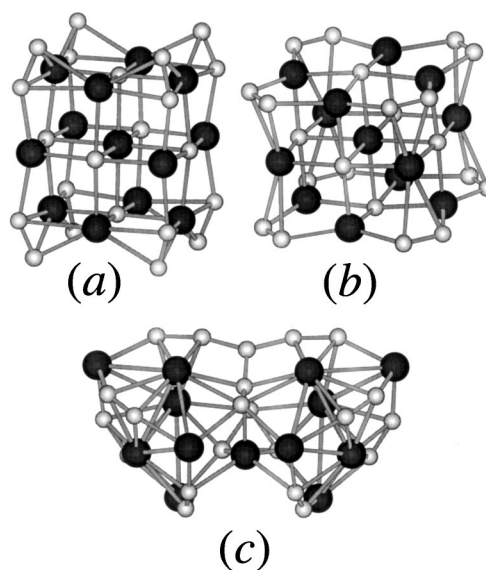


FIG. 1. Three optimized structures for the $Ti_{13}C_{22}$ cluster. (a) D_{4h} , cubic structure with eight C_2 dimers at the cube corners in slightly vertical positions; (b) D_{4h} , cubic structure with eight C_2 dimers at the cube corners in horizontal positions; (c) C_s , distorted structure resulting from an ideal double cage structure.

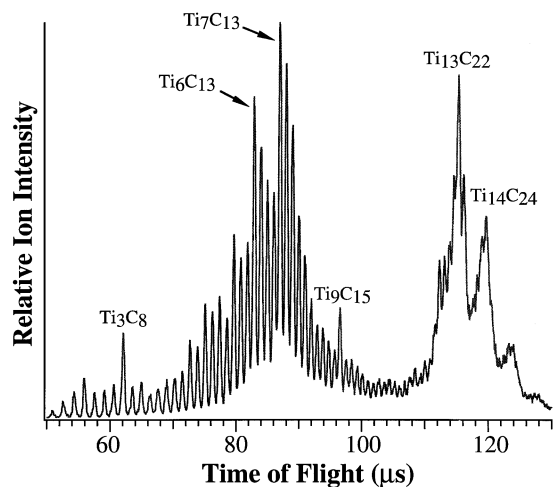


FIG. 2. Anion mass spectrum of titanium carbide clusters. Note the absence of the $\text{Ti}_8\text{C}_{12}^-$ metcar anion and the bimodal cluster distribution. The assignment of the exact cluster compositions is ascertained by using $^{13}\text{CH}_4$ isotope substitution.

anion mass spectrum. Instead, the anions exhibit a bimodal distribution where clusters containing eight to twelve Ti atoms show very low abundance, except $\text{Ti}_9\text{C}_{15}^-$ which displays a local magic number. Most interesting is the observation of the prominent $\text{Ti}_{13}\text{C}_{22}^-$ cluster, following the valley in the bimodal distribution. The peaks beyond the $\text{Ti}_{13}\text{C}_{22}^-$ cluster each show an increment by TiC_2 as shown in Fig. 2.

The magic $\text{Ti}_{13}\text{C}_{22}^-$ cluster must have exceptional stability. A critical question is whether the structure of the $\text{Ti}_{13}\text{C}_{22}^-$ cluster is the double cage. If it is, how is it formed since the single cage $\text{Ti}_8\text{C}_{12}^-$ is totally absent? Thus, the structure and bonding of the $\text{Ti}_{13}\text{C}_{22}$ cluster becomes the key to understanding the growth pathways of the large carbide clusters. We carried out a study that combined anion photoelectron spectroscopy (PES) and density functional calculations, in order to unravel the structure and bonding of the crucial $\text{Ti}_{13}\text{C}_{22}$ cluster. We measured PES spectra for all the cluster anions shown in Fig. 2. The spectrum of $\text{Ti}_{13}\text{C}_{22}^-$ is particularly interesting, showing several well-defined features between 3 and 4.5 eV with a characteristic energy gap around 5 eV (Fig. 3). To compare with the experiment, we calculated three possible structures of $\text{Ti}_{13}\text{C}_{22}$, including the double cage. Two important observations were taken into account in choosing alternative structures: (1) The importance of the C_2 dimer as found in the Ti_8C_{12} metcar [6–9], and (2) the cubic structural feature as shown in the cubic $\text{Ti}_{14}\text{C}_{13}$ cluster [5]. The previously observed $\text{Ti}_{14}\text{C}_{13}^+$ cluster is a $3 \times 3 \times 3$ cubic structure with eight metal atoms at the cube corners. However, a similar $\text{Ti}_{13}\text{C}_{14}^+$ cubic cluster with eight C atoms at the cube corners has never been observed. We noticed that replacing the eight corner C atoms in such a cubic cluster with eight C_2 dimers naturally leads to the

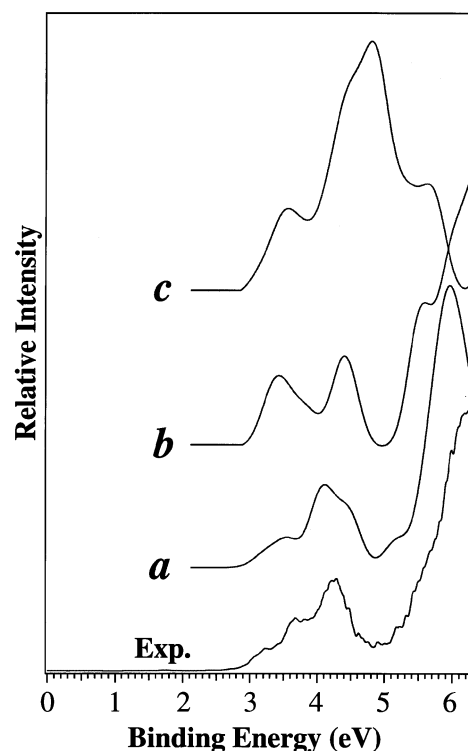


FIG. 3. Photoelectron spectrum of the $\text{Ti}_{13}\text{C}_{22}^-$ cluster at 193 nm (6.42 eV), compared with simulated electronic density-of-state spectra of the three optimized structures discussed in Fig. 1. Gaussian functions with a 0.02 eV width were used in the simulations.

$\text{Ti}_{13}\text{C}_{22}$ composition observed in Fig. 2. Hence, two such cubic structures with different C_2 orientations were also calculated.

The theoretical calculations were performed under both local spin density (LSD) and nonlocal spin density (NLSD) approximations. The LSD calculations used the Vosko-Wilk-Nusair local correlation functional [16] while the NLSD method employed Becke's gradient-corrected exchange functional [17] and Perdew-Wang's gradient-corrected correlation functional [18]. The non-local correction was incorporated in the SCF cycles in an iterative manner. Double numerical basis set augmented with polarization functions were used and all inner core electrons were frozen. The calculations were done using DMOL [19].

Our optimized geometries for the three structures are shown in Fig. 1. The geometry optimizations were carried out under imposed D_{4h} point group symmetry for (a) and (b) and C_s for (c). The binding energies for (a), (b), and (c) are 263.63, 261.63, and 262.30 eV, respectively, at the LSD level. The binding energies for (a) and (b) become 231.06 eV (6.60 eV/atom) and 229.30 eV (6.55 eV/atom), respectively, at the NLSD level. Because of the enormous computational effort, (c) was optimized only at the LSD level, and we expect that the ordering of the binding energies will remain the same.

The electron affinities, calculated only for (a) and (b), are both about 3.0 eV. We found that the structure (a) has the lowest energy. The double-cage metcar is totally distorted in the optimized structure (c), that shows similar bonding characteristics to the tetracapped tetrahedral Ti_8C_{12} structure [9].

To facilitate comparison with the experiment, we further simulated the electronic density of states (DOS) for each isomer using Gaussian functions. The simulated DOS spectra are compared with the PES spectrum in Fig. 3. The distorted double-cage structure can be easily ruled out. The calculated EAs for both (a) and (b) are about 3.0 eV, in excellent agreement with the experimental value (3.0 ± 0.1 eV). The simulated DOS spectra of (a) and (b) both reproduce well the characteristic energy gap at 5 eV. However, the overall agreement is seemingly better for the lowest energy (a) structure. It is possible that both (a) and (b) may be present. In fact, the difference between the two is rather small—rotating each structure by 90° and slightly displacing the C_2 dimers, one can convert (a) to (b) or vice versa.

The cubic $\text{Ti}_{13}\text{C}_{22}$ structure is interesting since it embodies two important bonding characteristics of the titanium carbide clusters: the C_2 dimers and the cubic structural framework. This indicates that indeed cubic structures are preferred for the large titanium carbide clusters: The simple cubic $\text{Ti}_{14}\text{C}_{13}^+$ cluster is formed in the cation channel, while the cubic $\text{Ti}_{13}\text{C}_{22}^-$ with eight C_2 dimers is formed in the anion channel. The previously observed $\text{Zr}_{13}\text{C}_{22}^+$ cluster is likely to be a cubic structure with eight C_2 dimers [4]. A challenging question concerning the cubic structures is whether they can explain systematically all the magic numbers previously attributed to the multicages. The answer is definitive.

The structure of $\text{Ti}_{13}\text{C}_{22}$ [Fig. 1(a)] is composed of three layers: two layers of Ti_4C_9 (A) sandwiching a layer of Ti_5C_4 (B). The stability of this structure derives from the fact that all the Ti atoms are optimally bonded to the C atoms and C_2 dimers. A growth pathway in which the A and B layers are stacked alternatively will reproduce all the magic numbers assigned to the multicages. The three-layer ABA cubic structure explains uniquely the observed $\text{Zr}_{13}\text{C}_{22}^+$ cluster. A five-layer ABABA structure gives a unique $M_{22}\text{C}_{35}$ composition (Fig. 4), corresponding to the observed $\text{Zr}_{22}\text{C}_{35}^+$ cluster explained as the quadruple cage closing [4]. A four-layer ABAB structure yields a composition of $M_{18}\text{C}_{26}$, which is three carbons short of the triple-cage $M_{18}\text{C}_{29}$ composition, observed as $\text{Zr}_{18}\text{C}_{29}^+$. We note that clusters with both capping A layers seem to make especially stable structures, as exemplified by the ABA structure, due to the optimized bonding of the metal atoms with the C_2 dimers. The B layer, which is carbon-deficient, seems to be susceptible to accumulating more carbons when not sandwiched. Thus it is not surprising that the $\text{Zr}_{18}\text{C}_{29}$ composition was observed instead of the ideal ABAB structure. This interpretation and

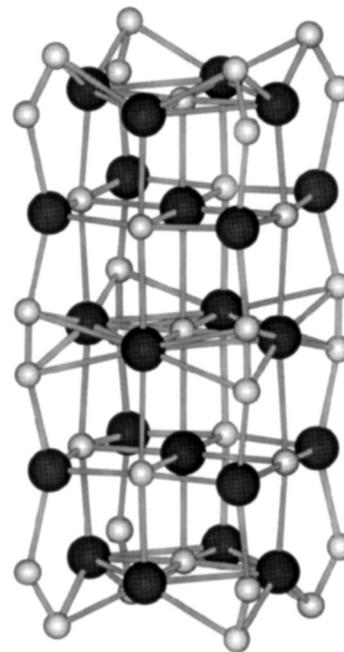


FIG. 4. Optimized structure of a five-layer ABABA structure ($\text{Ti}_{22}\text{C}_{35}$) with a total binding energy of 379.72 eV (6.66 eV/atom, NLSD). Further layered growth can lead to highly stable structures which form a class of novel one-dimensional quantum wires.

the layered growth path are further supported by the observation of the $\text{Ti}_9\text{C}_{15}^-$ magic number in the valley of the bimodal distribution in Fig. 2. An ideal two-layer AB cluster gives a $M_9\text{C}_{13}$ composition. The $\text{Ti}_9\text{C}_{15}^-$ cluster is likely composed of this ideal AB structure plus two extra C atoms, providing the precursor for the more stable ABA cluster.

Questions still remain about what controls the growth mechanisms. There seem to be distinct differences between the cations and anions in the titanium carbide system. Reddy and Khanna suggested that the formation of metcars or cubic $\text{Ti}_{14}\text{C}_{13}$ clusters depends on the C/Ti ratios in the cluster source: High C/Ti ratio favors the metcar formation due to abundant C_2 molecules [7]. Wei *et al.* showed that the formation of the $\text{Nb}_{13}\text{C}_{22}^+$ or the cubic $\text{Nb}_{14}\text{C}_{13}^+$ cluster is kinetically controlled and can be formed at different conditions [12]. We think that for the titanium carbide system hydrogen or certain hydrocarbon intermediates may also play a key role in the layered cubic growth involving C_2 dimers in the anions. We note that both C_2^- and C_2H^- and carbon clusters up to C_8^- are abundant in the plasma reactions.

We suspect that under certain experimental conditions the layered growth may allow very large $A(\text{BA})_n$ type of structures to be formed, with the $\text{Ti}_{13}\text{C}_{22}$ cluster being the $n = 1$ case. We also performed calculations for $n = 2$ (Fig. 4) and found it to be highly stable. This five-layer ABABA cluster ($\text{Ti}_{22}\text{C}_{35}$) has a similar electronic structure to that of $\text{Ti}_{13}\text{C}_{22}$, with a binding energy (6.66 eV/atom)

even higher than that of $\text{Ti}_{13}\text{C}_{22}$ (6.60 eV/atom). The energy gap near the Fermi level is rather small for these clusters and decreases as the length of the cluster increases (0.31 eV for $n = 1$ and 0.16 eV for $n = 2$). These clusters essentially form a class of novel one-dimensional metallic quantum wires which should exhibit novel transport properties depending on their lengths. These quantum wires may be produced in similar ways to that of the carbon nanotubes or formed on appropriate substrates. The C_2 dimers covering the surfaces of the quantum wires should also make them chemically stable.

We thank experimental assistance by Dr. S. Li. H. C. gratefully acknowledges Dr. P. M. Mathias for his support of this collaborative research. The theoretical work was done at Air Products and Chemicals, Inc. The support of this research by the National Science Foundation through a CAREER Program Award (No. DMR-9622733) to L. S. W. is gratefully acknowledged. The work is performed at Pacific Northwest National Laboratory, operated for the U.S. Department of Energy by Battelle under Contract No. DE-AC06-76RLO 1830.

-
- [1] B. C. Guo, K. P. Kerns, and A. W. Castleman, Jr., *Science* **255**, 1411 (1992); B. C. Guo *et al.*, *ibid.* **256**, 511 (1992).
- [2] J. S. Pilgrim and M. A. Duncan, *J. Am. Chem. Soc.* **115**, 6958 (1993).
- [3] H. Kroto *et al.*, *Nature (London)* **318**, 1662 (1985).
- [4] S. Wei *et al.*, *Science* **256**, 818 (1992).
- [5] J. S. Pilgrim and M. A. Duncan, *J. Am. Chem. Soc.* **115**, 9724 (1993); *Int. J. Mass Spectrom. Ion Process.* **138**, 283 (1994).
- [6] R. W. Grimes and J. D. Gale, *J. Chem. Soc. Chem. Commun.* 1222 (1992); T. T. Rantala *et al.*, *Z. Phys. D* **26**, 5255 (1992); L. Pauling, *Proc. Natl. Acad. Sci. U.S.A.* **89**, 8175 (1992); Z. Lin and M. B. Hall, *J. Am. Chem. Soc.* **114**, 10054 (1992); B. V. Reddy, S. N. Khanna, and P. Jena, *Science* **258**, 640 (1992); M. Methfessel *et al.*, *Phys. Rev. Lett.* **71**, 209 (1993); P. J. Hay, *J. Phys. Chem.* **97**, 3081 (1995); L. Lou *et al.*, *J. Chem. Phys.* **99**, 5301 (1993).
- [7] B. V. Reddy and S. N. Khanna, *Chem. Phys. Lett.* **209**, 104 (1993); *J. Phys. Chem.* **98**, 9446 (1994).
- [8] A. Ceulemans and P. W. Fowler, *J. Chem. Soc. Faraday Trans.* **88**, 2797 (1992); M. Rohmer, P. de Vaal, and M. Benard, *J. Am. Chem. Soc.* **114**, 9696 (1992); H. Chen *et al.*, *Phys. Rev. Lett.* **71**, 1732 (1993).
- [9] I. Dance, *J. Chem. Soc. Chem. Commun.* 1779 (1992); *J. Am. Chem. Soc.* **118**, 2699 (1996); **118**, 6309 (1996); M. Rohmer *et al.*, *ibid.* **117**, 508 (1995); *J. Chem. Soc. Chem. Commun.* 1182 (1993); *J. Phys. Chem.* **99**, 16913 (1995); Z. Lin and M. B. Hall, *J. Am. Chem. Soc.* **115**, 11165 (1993).
- [10] S. F. Cartier *et al.*, *Science* **260**, 195 (1993); S. Lee *et al.*, *Science* **267**, 999 (1995); L. S. Wang, S. Li, and H. Wu, *J. Phys. Chem.* **100**, 19211 (1996).
- [11] S. Wei *et al.*, *J. Phys. Chem.* **96**, 4166 (1992); *ibid.* **97**, 9559 (1993); B. D. May *et al.*, *Chem. Phys. Lett.* **242**, 265 (1995); S. F. Cartier, B. D. May, and A. W. Castleman Jr., *ibid.* **104**, 3423 (1996); *J. Phys. Chem.* **100**, 8175 (1996); K. P. Kerns *et al.*, *J. Am. Chem. Soc.* **116**, 4475 (1994).
- [12] S. Wei *et al.*, *J. Am. Chem. Soc.* **116**, 4475 (1994).
- [13] J. S. Pilgrim and M. A. Duncan, *J. Am. Chem. Soc.* **115**, 4395 (1993); **115**, 9724 (1993); J. S. Pilgrim, L. R. Brock, and M. A. Duncan, *J. Phys. Chem.* **99**, 544 (1995); L. R. Brock and M. A. Duncan, *ibid.* **100**, 5654 (1996).
- [14] Y. G. Byun, S. A. Lee, and B. S. Freiser, *ibid.* **100**, 14281 (1996); C. S. Yeh *et al.*, *J. Am. Chem. Soc.* **116**, 8806 (1994); Y. G. Byun and B. S. Freiser, *ibid.* **118**, 3681 (1996).
- [15] L. S. Wang, H. Cheng, and J. Fan, *J. Chem. Phys.* **102**, 9480 (1995); H. Wu, S. R. Desai, and L. S. Wang, *Phys. Rev. Lett.* **76**, 212 (1996).
- [16] S. J. Vosko, L. Wilk, and M. Nusair, *Can. J. Phys.* **58**, 1200 (1980).
- [17] A. D. Becke, *J. Chem. Phys.* **88**, 2547 (1988).
- [18] J. P. Perdew and Y. Wang, *Phys. Rev. B* **45**, 13244 (1992).
- [19] DMOL 95.0/3.0.0, Biosym/MSI, San Diego, CA, 1995.